



**HAL**  
open science

## Differential Evolution for Optimal Grouping of Condition Monitoring Signals of Nuclear Components

Piero Baraldi, Enrico Zio, Francesco Di Maio, Luca Pappaglione, R. Chevalier,  
R. Seraoui

► **To cite this version:**

Piero Baraldi, Enrico Zio, Francesco Di Maio, Luca Pappaglione, R. Chevalier, et al.. Differential Evolution for Optimal Grouping of Condition Monitoring Signals of Nuclear Components. ESREL 2011, Sep 2011, Troyes, France. pp.410-418. hal-00658087

**HAL Id: hal-00658087**

**<https://centralesupelec.hal.science/hal-00658087>**

Submitted on 12 Jan 2012

**HAL** is a multi-disciplinary open access archive for the deposit and dissemination of scientific research documents, whether they are published or not. The documents may come from teaching and research institutions in France or abroad, or from public or private research centers.

L'archive ouverte pluridisciplinaire **HAL**, est destinée au dépôt et à la diffusion de documents scientifiques de niveau recherche, publiés ou non, émanant des établissements d'enseignement et de recherche français ou étrangers, des laboratoires publics ou privés.

# Differential Evolution for Optimal Grouping of Condition Monitoring Signals of Nuclear Components

P. Baraldi, E. Zio, F. Di Maio & L. Pappaglione  
*Politecnico di Milano, Milano, Italy, E-mail: piero.baraldi@polimi.it*

R. Chevalier and R. Seraoui  
*Electricité de France – R&D, France*

**ABSTRACT:** We propose an approach for optimally grouping a large number of signals measured, for utilization in models for equipment condition monitoring. We use a Differential Evolution (DE) algorithm for the optimal identification of the groups; the decision variables of the optimization problem relate to the composition of the groups (i.e. which signals they contain) and the objective function (fitness) driving the search for the optimal grouping is constructed in terms of quantitative indicators of the performances of the condition monitoring models themselves: in this sense, the DE search engine functions as a wrapper around the condition monitoring models. A real case study is considered, concerning the condition monitoring of the Reactor Coolant Pump (RCP) of a nuclear Pressurized Water Reactor (PWR). The results of the grouping are evaluated with respect to the accuracy and robustness of the estimates of the monitored signals by the condition monitoring model developed on the optimal groups, and compared with those achieved with groups obtained using Genetic Algorithm wrapper approach.

**Keywords:** Condition Monitoring, Abnormal Condition Detection, Signal Grouping, Differential Evolution, Reactor Coolant Pump, Pressurized Water Reactor.

## 1 INTRODUCTION

For monitoring the condition of a component, a (typically empirical) model estimating the values of measurable signals in normal conditions is built; during operation, the measured values are compared with those estimated ('reconstructed') by the model: a deviation between the observed and reconstructed values reveals the presence of an abnormal condition (Reifman, J. 1997).

In practical industrial implementations, the performance of a single model estimating all the signals measured by the sensors, usually a very large number, may not be satisfactory. It has been shown that grouping the signals and then building a specialized model for each group allows to remarkably increase the condition monitoring performance (Roverso, D. et al. 2007; Baraldi, P. et al. 2010).

In this work, a Wrapper approach has been employed to group the signals: a search algorithm is used as a "wrapper" around the condition monitoring model; during the optimization search, the performance of the condition monitoring model itself is directly used as evaluation

function to compare the different groups selected by the search engine (Fig. 1).

The algorithm considered in this work for reconstructing the equipment behavior in normal conditions is based on the Auto-Associative Kernel Regression method (AAKR) (Hines, J.W. & Garvey D.R. 2006). AAKR is an empirical modeling technique that uses historical observations of the signals taken during normal plant operation.

We use the Differential Evolution (DE) algorithm as search engine for the identification of the optimal signal groups. The motivation of the choice is found in the DE ability of finding the optimal solution by efficiently scanning the search space in an acceptable computational time.

Differential Evolution is a derivation of Genetic Algorithms (Storn, R. & Price, K. 1995). DE applies evolution operations on the individuals' solutions of a population in order to perturb them by transmission of good properties, with the aim of finding an optimum. One difference with respect to GA is that DE is specifically built for optimization over continuous spaces and does so based on a floating-point representation. The specific evolutionary operations used in DE

are suited for such representation of the chromosomes, and drive the main improvements of DE with respect to GA. The DE-based wrapper approach is tested on a real case study concerning 46 signals selected among those used to monitor the reactor coolant pump of a Pressurized Water Reactor (PWR). The condition monitoring performance is evaluated with respect to metrics that measure i) the accuracy, i.e. the ability of the overall model to correctly and accurately reconstruct the signal values when the plant is in normal operation; ii) the robustness, i.e. the overall model ability to reconstruct the signal values in case of abnormal operation and consequent anomalous behavior of some monitored signals (Efron, B. 1983). The results are compared with those achieved by considering groups based on signal correlation and groups previously found in (Baraldi, P. et al. 2011) by using a GA wrapper approach.

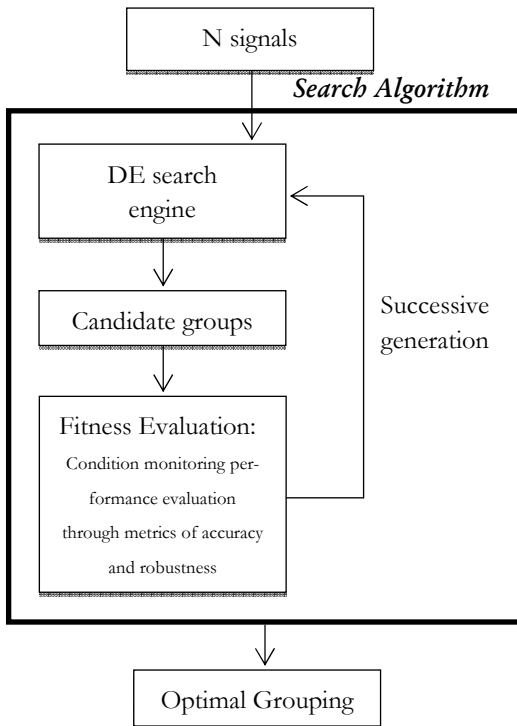


Figure 1. Wrapper approach for optimal signals grouping.

## 2 CONDITION MONITORING

Figure 2 shows a typical scheme of condition monitoring of a component. Sensor measurements  $\vec{x}^{obs}$  are sent to an auto-associative empirical model of the component behavior in normal condition (nc). Thus, the model provides in output the values expected in case of normal condition  $\vec{x}^{nc}$  of the input signals. A deviation between the measured  $\vec{x}^{obs}$  and reconstructed  $\vec{x}^{nc}$  values in one or more signals reveals the presence of faults (Reifman, J. 1997). In other words, in case of normal condition, the measured value  $\vec{x}^{obs} = \vec{x}^{obs-nc}$  should be very similar to the model reconstructions  $\vec{x}^{nc}$ , whe-

reas in case of abnormal condition (ac) the model still reconstructs  $\vec{x}^{nc}$ , which differs from the measured values  $\vec{x}^{obs} = \vec{x}^{obs-ac}$ . Notice that one usually does not know whether the component is working in normal or abnormal conditions, i.e. if  $\vec{x}^{obs} = \vec{x}^{obs-nc}$  or  $\vec{x}^{obs} = \vec{x}^{obs-ac}$ , whereas, by observing the residuals  $\vec{r} = \vec{x}^{obs} - \vec{x}^{nc}$ , it is possible to detect the component condition. In this respect, several methods of analysis of the residuals  $\vec{r}$  for fault detection exist, e.g. the Sequential Probability Ratio Test (SPRT) (Hines, J.W. & Garvey D.R. 2006). The model considered in this work for reconstructing the component behavior in normal condition is based on the AAKR method (Hines, J.W. & Garvey D.R. 2006). The basic idea of the method is to reconstruct, using historical observations, the signal values in case of normal condition,  $\vec{x}^{nc}$ , given a current signal measurement vector,  $\vec{x}^{obs} = (x^{obs}(1), \dots, x^{obs}(n))$ , as a weighted sum of the historical observations. Appendix A provides the details of the method.

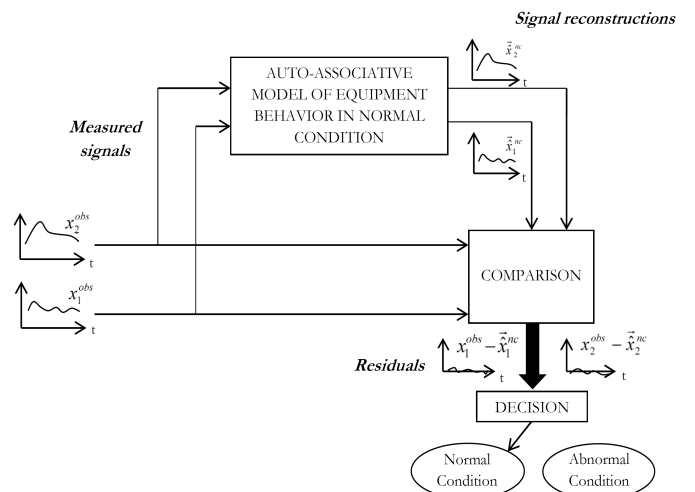


Figure 2. Condition monitoring scheme.

## 3 DIFFERENTIAL EVOLUTION

DE is an optimization method aiming at finding the global optimum of a set of real objective functions,  $F \equiv \{f(\cdot)\}$ , of one or more decision variables,  $U \equiv \{u\}$ , possibly subject to various linear or non linear constraints.

DE has emerged from Price's attempts to solve the Chebychev polynomial fitting problem posed to him by Storn (Storn, R. & Price, K. 1995). The analogies between DE and real-coded GA are several, but the shrewdnesses adopted by the novel operations of DE are the strengths of the DE technique.

The revolutionary idea of DE lies in the perturbation of the current population: this is obtained by adding to a chromosome the weighted difference between two others randomly selected from the population.

This is the original scheme proposed in (Storn, R. & Price, K. 1997): at the  $G^{\text{th}}$  generation, for each vector  $\underline{x}_{i,G}$  in the population, called target vector, a noisy vector  $\underline{v}_i$  is generated randomly choosing three mutually different vector indices  $r_1 r_2 r_3 \in \{1, 2, \dots, NP\}$  with  $1 \notin \{r_1 r_2 r_3\}$

$$\underline{v}_{i,G} = \underline{x}_{r_1,G} + F \cdot (\underline{x}_{r_2,G} - \underline{x}_{r_3,G}) \quad (1)$$

where the weighting (or scaling) factor  $F \in [0, 2]$  is a user-defined parameter, kept constant during the optimization. This operation is termed *mutation* in DE.

Using the weighted difference, the entire process becomes self-organized because the step length for the perturbation is mainly affected by the progress state of the evolutionary process. Through the evolution, the search space contracts or expands if the direction taken by the algorithm is correct or wrong, so the random step-length is self-adapted in every dimension accordingly with the dependence of the variable.

After *mutation*, the noisy vector is not directly compared with the target vector, but it is further modified by the *crossover* process, in which the noisy and target vectors are mixed according to some rule to create the trial vector  $\underline{u}_i$ , which inherits from them different pieces of chromosome. The *crossover* operator contributes to maintaining diversity inside the perturbed population, shuffling old and new information. This increases the probability of maintaining some good property from the target vector, and avoids drastic changes during the generation of new solutions. On the other hand, the role of *crossover* in DE has a secondary relevance compared to GA (Storn, R. & Price, K. 1995). Due to the chromosome vectorial representation, as for real-coded GA, the *crossover* operator for DE is applied to each element of the array: each variable of the noisy vector and the target vector has the possibility to be part of the trial vector, entering the final fight for survival. The most common crossover type adopted is the binomial approach: the trial vector is built by the following rule, gauged by a control parameter  $CR \in [0, 1]$ , which influences the probability that a noisy vector's variables are selected for the mutation process.

$$u_{ji,G} = \begin{cases} v_{ji,G} & \text{if } U(0,1) \leq CR \text{ or } j = \text{irand}(NP) \\ x_{ji,G} & \text{if } U(0,1) > CR \text{ and } j \neq \text{irand}(NP) \end{cases} \quad (2)$$

$$\forall j \in \{1, 2, \dots, n\}$$

where  $U(0,1)$  is a uniform continuous random value  $\in [0, 1]$ , whereas  $\text{irand}(NP)$  is a uniform

discrete random number in the set  $\in \{1, 2, \dots, NP\}$ .

This ruling applied to the Bernoulli trials guarantees the inheriting of at least one element from the noisy vector in the trial vector even if the crossover rate  $CR$  is set to zero. The binomial crossover operator acts independently on every "gene", i.e. variable of the chromosome, as for classic GA multi-site crossover. A relevant difference with GA is that in the DE *crossover* procedure a chromosome of the current population and one just generated, the noisy vector, are mixed, rather than two solutions of the population. The resulting trial vector

$$\underline{u}_{i,G} = (u_{1i,G}, u_{2i,G}, \dots, u_{ni,G}) \quad (3)$$

inherits portions from the noisy vector and from the target vector, as regulated by the parameter  $CR$ .

The trial vector obtained then enters the *selection* process where it is compared with the target vector  $\underline{x}_{i,G}$ , that is partially its parent according with the crossover rule. During the selection process, the population  $S$  is modified by substitution.

Referring to a Single Objective (SO) problem aiming at minimizing a single function  $f$ , if the trial vector's fitness is less than the target vector's fitness, the first will be a member of the next generation, replacing the target vector in the set  $S$ , and the trial vector is discarded:

$$\underline{x}_{i,G+1} = \begin{cases} \underline{u}_{i,G} & \text{if } f(\underline{u}_{i,G}) < f(\underline{x}_{i,G}) \\ \underline{x}_{i,G} & \text{otherwise} \end{cases} \quad (4)$$

$$\forall i \in \{1, 2, \dots, NP\}$$

The *selection* criterion in DE is greedy and quite different from the classical replacement criterion of GA: for sure the next generation will be better or at least equal to the previous generation.

The evolution of the DE algorithm follows these steps:

1. creation of an initial population of  $NP$  potential solutions and evaluation of their fitnesses;
2. for each solution of the population (target vector), selection of three solutions for reproduction;
3. for each target vector, creation of a noisy vector using the mutation process;
4. creation of a trial vector mixing target and noisy vectors;
5. comparison between each target vector and its related trial, and eventual replacement;

6. control of the stopping criteria: if some criterion is met, then stop, else return to step 2.

The stopping criteria adoptable are the same as for GA. DE has been shown to have robustness, higher convergence speed than GA and even superior accuracy thanks to its greedy search preference.

#### 4 APPLICATION

A real case study concerning 46 signals used to monitor the Reactor Coolant Pumps (RCPs) of a French PWR is considered. A dataset containing the signals values measured every hour for a period of 11 consecutive months has been considered to build the reconstruction model. To this purpose, the 46-dimensional available patterns (5798) have been divided into a set  $X_S$  of 2798 patterns used to perform the DE optimization, i.e. to find the optimal grouping, and a validation set  $X_V$  of 3000 patterns used to validate the condition monitoring performance of the grouping found. To this purpose a cross validation procedure has been performed on the patterns of  $X_V$  order to accurately estimate the values of the performance metrics, in particular, a “4-fold” cross-validation error estimate is used. To this purpose, the original dataset is randomly partitioned into 4 blocks of equal size. One of these blocks is used as validation data subset for the evaluation of the performance metrics of interest, and the remaining three blocks are combined together to constitute the training data subset. The cross-validation process is then repeated 4 times, each time using a different block as validation set (Efron, B. & Tibshirani, R.J. 1995; Kohavi, R. 1995). The objective of the search has been the minimization of a function which takes into account both the accuracy and the robustness of the grouping.

The accuracy, i.e. the ability of the model to reconstruct correctly the signal values in normal plant behavior, has been measured by considering the metric  $\overline{A_{ac}^{auto}}$ , which is the global accuracy obtained applying the disturbance to all the signals. An accurate condition monitoring model allows to reduce the number of false alarms, i.e. detections of faulty behaviors when no faulty conditions are actually occurring. The accuracy metric is typically defined as the mean square error (MSE) between the model reconstruction and the signal measured values. In this work, according to the (Zaharie, D. 2007), the metric  $\overline{A_{ac}^{auto}}$  has been chosen, instead the MSE, because has been seen that using this metric as fitness function in the search engine allows to obtain a signal grouping which is able to achieve higher accuracy when applied to all

data than with a little data set used to performing the search. This is due to the fact that the two metrics, MSE and  $\overline{A_{ac}^{auto}}$ , differs only for the signal values which are disturbed in case of  $\overline{A_{ac}^{auto}}$ , running a cross-validation procedure, while MSE is performed with all signals value in normal condition.

The accuracy in the reconstruction of the disturbed signal  $i$  is defined as:

$$A_{ac(i)}^{auto} = \frac{1}{N^{test}} \sum_{k=1}^{N^{test}} (\hat{X}_{nc}^{test-ac(i)}(k,i) - X^{test-nc}(k,i))^2 \quad (5)$$

This metric measures the mismatch between signal reconstructions and signal values in normal plant operation. However, since it does not consider neither the difference between the reconstructions in the cases of disturbed and undisturbed signals, nor the magnitude of the signal deviation ( $X^{test-ac(i)}(k,i) - X^{test-nc}(k,i)$ ) it cannot be directly interpreted as a measure of model robustness.

The robustness, i.e. the capacity to reconstruct properly the signals value when an anomaly occurs to the component has been measured by the metric  $\overline{S_{ac}^{auto}}$ , which is the global robustness obtained applying the disturbance to all the signals. In abnormal plant conditions, a robust model reconstructs the value of a plant signal as if the plant were in normal operation: then, the differences between the measured and the reconstructed signal values can easily identify the abnormal condition.

In this respect, real data measured by the sensors in abnormal plant conditions are usually not available because these latter are rare; then simulation is used to artificially inject abnormality by adding realistic deviations to the signals measured during normal plant operation. Let  $X^{obs-ac(i)}$  be a matrix of test patterns whose values of the  $i$ -th signal have been disturbed with deviations, with  $X^{obs-ac(i)}(k,j)$  indicating the value of the  $j$ -th signal of the  $k$ -th test pattern,  $k=1, \dots, N^{test}$ , and  $\hat{X}_{nc}^{test-ac(i)}(k,j)$  its reconstruction provided by the condition monitoring model which is expected to be the signal value in normal condition  $X^{test-nc}(k,j)$ .

Quantitative indicators of robustness can then be introduced as follows. The auto-sensitivity of the model to a disturbance applied on signal  $i$  is defined as (Efron, B. 1983):

$$S_{ac(i)}^{auto} = \frac{1}{N^{test}} \sum_{k=1}^{N^{test}} \left| \frac{\hat{X}_{nc}^{test-ac(i)}(k,i) - \hat{X}_{nc}^{test-nc}(k,i)}{X^{test-ac(i)}(k,i) - X^{test-nc}(k,i)} \right| \quad (6)$$

This metric measures the ability of the model to provide the same reconstructions in the two cases of disturbed or undisturbed signal  $i$ . In this respect, notice that a model characterized by a very low accuracy (high MSE) and very

high robustness (small  $S_{ac(i)}^{auto}$ ) is not satisfactory for condition monitoring since it still provides signal reconstructions very different from signal values in normal plant operation.

These two metrics actually measure errors and, thus, low values are desired. Global accuracy and robustness measures  $A_{ac}^{auto}$  and  $S_{ac}^{auto}$ , respectively, are then obtained by applying a disturbance to all the signals, computing the  $A_{ac(i)}^{auto}$  and  $S_{ac(i)}^{auto}$ , and finally taking, respectively, their mean values:

$$\overline{A_{ac}^{auto}} = \frac{\sum_{i=1}^q A_{ac(i)}^{auto}}{q} \quad (7)$$

$$\overline{S_{ac}^{auto}} = \frac{\sum_{i=1}^q S_{ac(i)}^{auto}}{q} \quad (8)$$

For the grouping optimization problem, single objective (SO) function is obtained by aggregation of the two metrics as follows:

$$f_{agg} = \overline{S_{ac}^{auto}} \cdot \overline{A_{ac}^{auto}} \quad (9)$$

In the next Section, the results obtained by the ‘wrapper’ scheme of Figure 2 with DE search engine are presented. As chromosomes, we simply take  $n$ -dimensional vectors of positive integers  $r \in \{1, R\}$ , where  $n$  is the number of monitored signals and  $R$  is the maximum number of groups reached by the DE: the integer value  $R_j$  of the  $j$ -th element of the vector indicates the group to which the  $j$ -th signal is assigned (Fig. 3).

GENE	signal 1	signal 2	...	signal $j$	...	signal $n$
GROUP						
LABEL (integer number)	$r_1$	$r_2$	...	$r_j$	...	$r_n$

↑  $1 \leq r_j \leq R = \text{maximum number of groups}$

Figure 3. Chromosome structure.

In our application,  $R$  has been taken equal to 5 as in (Baraldi, P. et al. 2011), in order to allow a fair comparison between the results achieved by the DE and the GA wrapper approaches. The crossover rate  $CR$  is set to 0.8 to adequately explore the search space, since it is very complex. The role of scaling factor is heavily significant in the convergence speed and success, with values under 0.15 success is not guaranteed and values over 0.5 the convergence speed slows down gradually. According to the recommendations reported in (Storn, R. & Price, K. 1997; Zaharie, D. 2007) the scaling factor  $F$  is set to 0.5.

## 5 RESULTS

### 5.1 Simulation Pure DE

Table 1 reports the DE parameters used:

Table 1. DE parameters.

Population size	50
Maximum number of generation	500
Scaling factor (F)	0.5
Crossover rate (CR)	0.8
Number of patterns in the training set	500
Number of patterns in the validation set	170
Gene possible values	[1,2,3,4,5]

Notice that the optimization problem of identifying the best group for each one of the 46 signals requires a search in a very large search space formed by  $5^{46} \approx 10^{32}$  possible solutions. For this reason, large number of generations (500) has been chosen for convergence of the DE to a satisfactory solution.

After 300 generations, the whole population is basically converging:  $\overline{S_{ac}^{auto}}$  slightly increases after generation 250, whereas  $\overline{A_{ac}^{auto}}$  tends to monotonously decrease. This is due to the fact that the optimization is based on the minimization of a single fitness function which aggregates the two accuracy and robustness metrics (eq. 9), and thus a slight increasing of the robustness can be compensated by a decreasing of the accuracy.

In this respect, optimization approaches in the framework of the Pareto analysis based on Multi-Objective Differential Evolution (MODE), could be explored to find a set of optimal solutions characterized by different compromises between accuracy and robustness. The groups obtained by the single-objective DE search are reported in Appendix B. Table 3 (columns 2) reports the performances obtained by the best solution found by the DE. These results are compared with those obtained by grouping the signals according to their correlation, i.e. by assigning to the same group the signals with an absolute value of the correlation coefficient larger than 0.8 (Baraldi, P. et al. 2010). Following this procedure, 4 groups have been identified, whereas the remaining 4 signals, characterized by a correlation coefficient with all other signals lower than 0.8, have been put together in a fifth group of uncorrelated signals (Appendix C).

Although the two groupings are characterized by very similar values of  $f_{agg}$ , they have different behaviors in terms of accuracy and robustness with the DE grouping being more robust but less accurate.

## 5.2 Simulation Hybrid DE

To improve  $\overline{A_{ac}^{auto}}$ , we consider the opportunity of reducing the DE search space by decreasing the number of signals that must be reorganized in groups.

To this purpose, it has been observed that out of the 46 signals the correlation grouping builds a group formed by 30 highly correlated temperature signals that enables a very accurate and robust reconstruction of 24 of these 30 signals. Then we have decided to adopt an hybrid approach which consists in keeping these 24 signals in a group (i.e. group 1) and using the DE search to optimize the group assignment of the remaining 22 signals. The correlating chromosome is formed by a vector of 22 elements (the signals which should be assigned to a group) which can take a value between 1 and 5 (the group to which the signal is assigned). We observe that one of the group to which the signals can be assigned is the group of the 24 signals identified by the correlation grouping itself. In this way, the dimension of the search space is reduced from the  $5^{46} (\approx 10^{32})$  possible combinations to  $5^{24} (\approx 10^{17})$ . Table 2 reports the DE parameters used within this hybrid approach.

With the reduced dimension of the search space, the number of generations has been reduced to 250 leading to a reduction of the computational time.

Appendix D reports the groups obtained by the hybrid approach. With respect to the correlation grouping one can notice that:

- groups 1 and 4 are identical in the two grouping approaches;
- the other three groups differ only with respect to signals 10a and 10d, which are assigned to groups 2 and 5 by the hybrid approach and to group 3 by the correlation grouping.

Table 2. Hybrid DE parameters.

Population size	50
Maximum number of generation	250
Scaling factor (F)	0.5
Crossover rate (CR)	0.8
Number of patterns in the training set	500
Number of patterns in the validation set	250
Gene possible values	[1,2,3,4,5]

Figures 4-6 show the evolution of the fitness function  $f_{agg}$ , the metrics  $\overline{A_{ac}^{auto}}$  and  $\overline{S_{ac}^{auto}}$ , respectively, with the number of generations. The mean and best fitness at the first generation are lower (0.0103 and 0.0062) than those previously obtained in the previous search (0.0125 and 0.0095). This is due to the fact that in the hybrid correlation and DE approach, the pres-

ence of a high performing group composed by 24 signals is guaranteed. With respect to the global improvement between the first and the last generation, in the hybrid approach, DE has been able to reduce the fitness of the best individual of about 50%, i.e.  $(f_{agg}^{(1)} - f_{agg}^{(250)}) / f_{agg}^{(1)} \approx 50\%$ .

The robustness of the solutions tends to remarkable decrease after generation 200 (Fig. 6). This behavior, which is found also in the pure DE search, is in this case more remarkable given that the robustness decreases of about 30%.

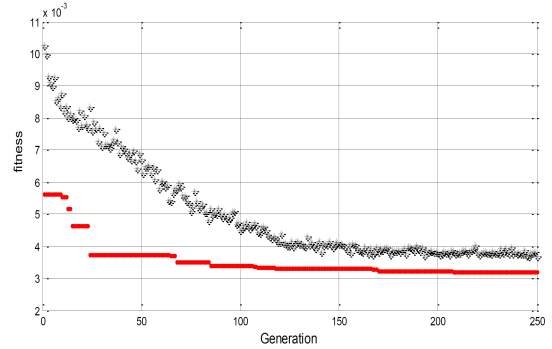


Figure 4. Evolution of the best (x) and mean (.) population fitness value at each generation.

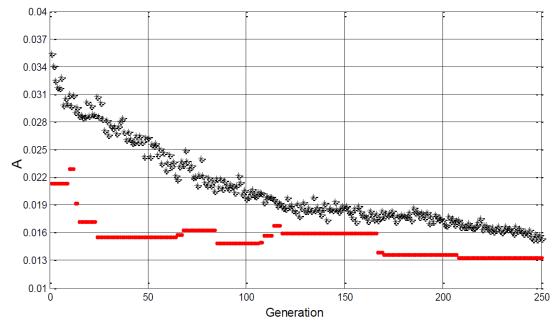


Figure 5. Evolution of the best (x) and mean (.) accuracy value at each generation.

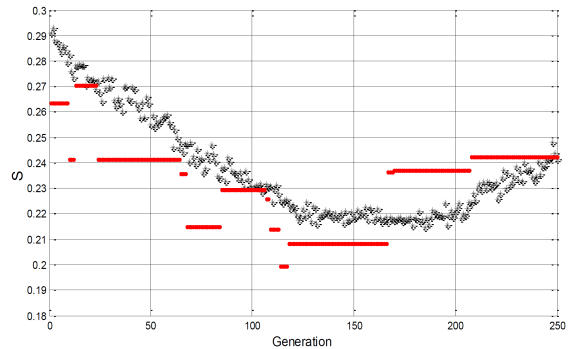


Figure 6. Evolution of the best (x) and mean (.) robustness value at each generation.

Table 3 (column 4) reports the performances of the grouping found by the hybrid approach. The fitness results are lower than those obtained by the correlation grouping and pure DE approach. With respect to the correlation grouping, the DE allows finding a solution with about the same accuracy but more robust.

### 5.3 Comparison with a GA wrapper approach

In this Section, we compare the performance of the grouping obtained by DE with that obtained by GAs in (Baraldi, P. et al. 2011). First of all, notice that GAs are not able to find a satisfactory solution in the case in which the search space is formed by all the possible combinations of the 46 signals, the fitness of the best grouping being equal to 0.0095.

Using an hybrid correlation and GAs approach, where, analogously to what is done in the hybrid correlation and DE approach, the 24 highly correlated temperature signals are kept in a fixed group, we have obtained a grouping characterized by the performances reported in Table 3.

Table 3. Performances of the different grouping methods.

Grouping metrics	Correlation	Pure DE
$\bar{A}$	$0.00833 \pm 0.00066$	$0.01173 \pm$
$\bar{S}$	$0.29719 \pm 0.00573$	$0.22515 \pm$
$f_{agg}$	$0.00247 \pm 0.00025$	$0.00264 \pm$
Grouping metrics	Hybrid DE	Hybrid GA
$\bar{A}$	$0.00867 \pm 0.00062$	$0.00861 \pm$
$\bar{S}$	$0.26781 \pm 0.00282$	$0.28927 \pm$
$f_{agg}$	$0.00229 \pm 0.00017$	$0.00248 \pm$

The solution found by the hybrid DE and correlation approach is more performing than that found by the hybrid GAs and correlation approach with respect to robustness, for approximately the same accuracy.

The groupings found by the two approaches (Appendixes D and E) differ only for the assignment of signals 10a and 10d which are two flow measurement signals characterized by a low correlation with all other 44 signals.

In order to compare the robustness of the groupings found by the two hybrid approaches, the reconstructions of signals 10d are compared in case of abnormal conditions. The abnormal conditions have been simulated by adding a linear drift to the signal values collected for 100 hours in normal conditions. Figure 7 shows the signal 10d behavior in case of normal conditions (top) and abnormal conditions (bottom). The signal values in abnormal conditions are then given in input to the AAKR reconstruction models. Figure 8 (top) shows the reconstructions obtained by using the hybrid

GA and correlation grouping and Figure 9 (top), the hybrid DE and correlation grouping.

Finally, Figure 8 (bottom) and Figure 9 (bottom) show the difference between the abnormal condition measurement and the reconstruction, which is used for the abnormal condition detection. Notice that after 60 hours the signal 10d reconstruction obtained by the hybrid DE and correlation grouping tends to be different from the abnormal condition measurement, allowing to identify the onset of an abnormal condition. On the contrary, the identification of the abnormal conditions results difficult using the hybrid correlation and GA grouping, given that the residuals between the signal measurement in abnormal conditions and the reconstruction do not remarkable deviate from zero.

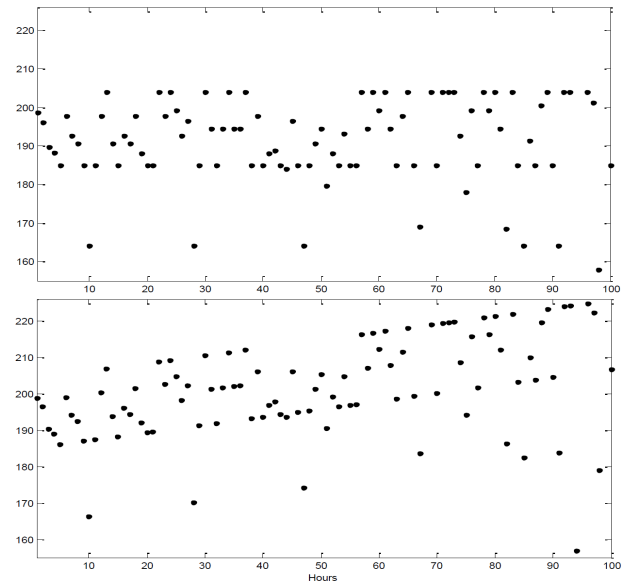


Figure 7. Time evolution of signal 10d in normal condition during 100 consecutive hours (top); time evolution of signal 10d in abnormal condition, linearly drifted by 0.7% of the standard deviation.

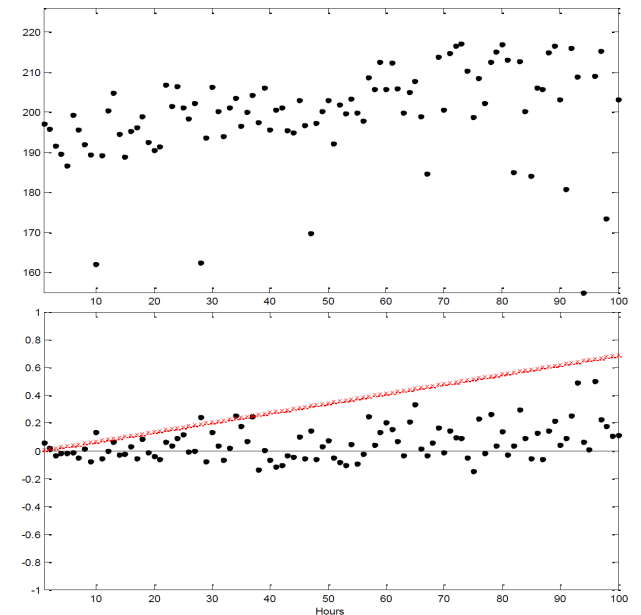


Figure 8. GA grouping. Reconstruction performed of signal 10d in abnormal condition, linearly drifted by 0.7% of

the standard deviation (top); difference with respect abnormal conditions (solid line) and normal conditions (crosses) (bottom).

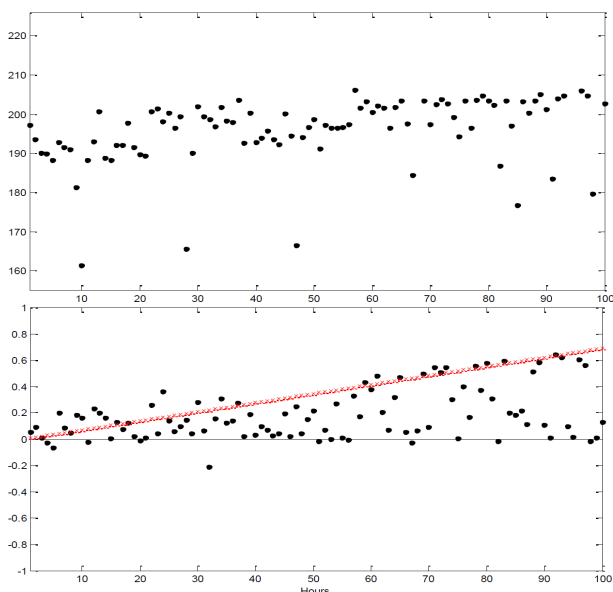


Figure 9. DE grouping. Reconstruction performed of signal  $10d$  in abnormal condition, linearly drifted by 0.7% of the standard deviation (top); difference with respect abnormal conditions (solid line) and normal conditions (crosses) (bottom).

## 6 CONCLUSION

In this paper, we have proposed an approach to optimal grouping for condition monitoring, based on a wrapper DE search approach. The approach has been applied to the condition monitoring of 46 RCP signals. The objective of the search has been to minimize a proper objective function which takes into account both the accuracy and robustness of the signal reconstructions. The obtained grouping has resulted more performing than that obtained by grouping the signals according to their correlation, or using a previously developed wrapper GA approach. We intend to continue our research work focusing on grouping approaches based on Multi-Objective Differential Evolution (MODE) optimization techniques in the framework of Pareto analysis. These approaches are expected to provide a set of optimal solutions characterized by different compromises between accuracy and robustness. Using these approaches, one can choose the solution with the most satisfactory tradeoff between the two objectives.

## ACKNOWLEDGMENT

This research has been carried out under contract C935C50010 funded by EdF R&D.

## REFERENCES

- Baraldi, P., Canesi, R., Zio, E., Seraoui, R. & Chevalier, R. 2010. Signal Grouping for Condition Monitoring of Nuclear Power Plant Components, *Control and Human-Machine Interface Technologies NPIC&HMIT*, Seventh American Nuclear Society International Topical Meeting on Nuclear Plant Instrumentation, on CD-ROM, American Nuclear Society, LaGrange Park. Las Vegas: Nevada.
- Baraldi P., Canesi, R., Zio, E., Seraoui, R. & Chevalier, R. 2011. Generic algorithm-based wrapper approach for grouping condition monitoring signal of nuclear power plant components, Submitted to *Integrated Computer-Aided Engineering*.
- Efron, B. 1983. Estimating the error rate of a prediction rule: Improvement on cross-validation. *American Statistical Association* 78 (382): 316-331.
- Efron, B. & Tibshirani, R.J. 1995. Improvements on cross-validation: The .632+ bootstrap method. *American Statistical Association*, 92 (43): 548-560.
- Hines, J.W. & Garvey, D.R. 2006. Development and Application of Fault Detectability Performance Metrics for Instrument Calibration Verification and Anomaly Detection. *Pattern Recognition Research* 1: 2-15.
- Kohavi, R. 1995. *A Study of Cross-Validation and Bootstrap for Accuracy Estimation and Model Selection*. San Mateo: California: Morgan Kaufman: 1137-1143.
- Reifman, J. 1997. Survey of artificial intelligence methods for detection and identification of component faults in nuclear power plants. *Nuclear Technology* 119: 76-97.
- Roverso, D., Hoffmann, M., Zio, E., Baraldi, P. & Gola, G. 2007. Solutions for plant-wide on-line calibration monitoring. *ESREL* 1: 827-832, Stavanger: Norway.
- Storn, R. & Price, K. 1995. Differential evolution - A simple and efficient adaptive scheme for global optimization over continuous spaces. *Technical Report TR-95-012 International Computer Science Institute*. Berkeley: California.
- Storn, R. & Price, K. 1997. Differential evolution - A simple and efficient heuristic for global optimization over continuous spaces. *Global Optimization* 11: 341-359.
- Zahine, D. 2007. A Comparative Analysis of Crossover Variants in Differential Evolution. U. Markowaska-Kaczmar and H. Kwasnicka, Wisla (eds.), *Proceeding of IMCSIT 2007*: 171-181.

## APPENDIX A: AUTO-ASSOCIATIVE KERNEL REGRESSION METHOD

Let  $X^{obs-nc}$  be a matrix of observed data whose generic element  $X^{obs-nc}(k, j)$  represents the  $k$ -th time observation,  $k=1, \dots, N$ , of the  $j$ -th measured signal,  $j=1, \dots, q$ , taken during normal plant condition. The basic idea of the method is to reconstruct the signal values in case of normal condition,  $\hat{x}^{nc}$ , given a current signal measurement vector,  $\bar{x}^{obs} = (x^{obs}(1), \dots, x^{obs}(q))$ , as a weighted sum of the observations in  $X^{obs-nc}$ .

Thus,  $\hat{x}^{nc}(j)$ , the reconstruction of  $x^{obs}(j)$ , the  $j$ -th component of  $\bar{x}^{obs}$ , is given by:

$$\hat{x}^{nc}(j) = \frac{\sum_{k=1}^N w(k) \cdot X^{obs-nc}(k, j)}{\sum_{k=1}^N w(k)} \quad (A1)$$

The weights  $w(k)$  are similarity measures obtained by computing the Euclidean distance between the current sensor measurements  $\bar{x}^{obs}$  and the  $k$ -th observation of  $X^{obs-nc}$ :

$$d^2(k) = \sum_{j=1}^q (x^{obs}(j) - X^{obs-nc}(j, k))^2 \quad (A2)$$

and inserting it in the Gaussian kernel:

$$w(k) = \frac{1}{\sqrt{2\pi}h} e^{-\frac{d^2(k)}{2h^2}} \quad (A3)$$

where the signal  $h$  defines the Gaussian bandwidth.

In order to provide in Eq. (A2) a common scale across the different signals measuring different quantities, it is necessary to normalize their values. In the present work, the signal values are normalized according to:

$$x_n(j) = \frac{x(j) - \mu(j)}{\sigma(j)} \quad (A4)$$

where  $x(j)$  is a generic measurement of signal  $j$  and  $\mu(j)$  and  $\sigma(j)$  are the mean and standard deviation of the  $j$ -th signal in  $X^{obs-nc}$ .

## APPENDIX B: PURE DE GROUPING

Group 1: 04a, 05a, 07a, 04b, 05b, 07b, 04c, 05c, 07c, 04d, 05d, 07d, 17, 20, 31a, 31b, 31c, 31d

Group 2: 09a, 12a, 13a, 14a, 09b, 12b, 13b, 14b, 09c, 12c, 13c, 14c, 09d, 12d, 13d, 14d, 29a, 29b, 29c, 29d

Group 3: 08a, 08b, 08c, 08d, 10a

Group 4: 10b, 10c, 10d

## APPENDIX C: CORRELATION GROUPING

Group 1: 04a, 05a, 07a, 09a, 12a, 13a, 14a, 04b, 05b, 07b, 09b, 12b, 13b, 14b, 04c, 05c, 07c, 09c, 12c, 13c, 14c, 04d, 05d, 07d, 09d, 12d, 13d, 14d, 17, 20

Group 2: 08a, 08b, 08c, 08d

Group 3: 10a, 10b, 10c, 10d

Group 4: 29a, 29b, 29c, 29d

Group 5: 31a, 31b, 31c, 31d

## APPENDIX D: HYBRID DE

Group 1: 04a, 05a, 07a, 09a, 12a, 13a, 14a, 04b, 05b, 07b, 09b, 12b, 13b, 14b, 04c, 05c, 07c, 09c, 12c, 13c, 14c, 04d, 05d, 07d, 09d, 12d, 13d, 14d, 17, 20

Group 2: 08a, 08b, 08c, 08d, 10a

Group 3: 10b, 10c

Group 4: 29a, 29b, 29c, 29d

Group 5: 31a, 31b, 31c, 31d, 10d

## APPENDIX E: HYBRID GA

Group 1: 04a, 05a, 07a, 09a, 12a, 13a, 14a, 04b, 05b, 07b, 09b, 12b, 13b, 14b, 04c, 05c, 07c, 09c, 12c, 13c, 14c, 04d, 05d, 07d, 09d, 12d, 13d, 14d, 17, 20

Group 2: 08a, 08b, 08c, 08d

Group 3: 10a, 10b, 10c

Group 4: 29a, 29b, 29c, 29d, 10d

Group 5: 31a, 31b, 31c, 31d